ORIGINAL ARTICLE

The Response of Glucose–Excited Neurones in the Ventromedial Hypothalamus to Decreased Glucose is Enhanced in a Murine Model of Type 2 Diabetes Mellitus

V. E. Cotero,* B. B. Zhang† and V. H. Routh*

Department of Pharmacology and Physiology, New Jersey Medical School (UMDNJ), Newark, NJ, USA.
†*Department of Metabolic Disorders, Merck Research Laboratories, Rahway, NJ, USA.*

Journal of
Neuroendocrinology

Correspondence to:
Vanessa H. Routh, Department of Pharmacology and Physiology, New Jersey Medical School (UMDNJ), PO Box 1709, Newark, NJ 07101-1709, USA (e-mail: routhvh@umdnj.edu).

Obesity and type 2 diabetes mellitus (T2DM) are associated with dysfunctional insulin signalling and impaired central glucose sensing. Glucose sensing neurones reside in key areas of the brain involved in glucose and energy homeostasis (e.g. ventromedial hypothalamus; VMH). We have recently shown that insulin attenuates the ability of glucose-excited (GE) neurones to sense decreased glucose. We hypothesise that this effect of insulin on VMH GE neurones is impaired during T2DM when insulin signalling is dysfunctional. To test our hypotheses, we used whole cell patch clamp recording techniques to evaluate the effects of insulin on VMH GE neurones in brain slices from wild-type and diabetic (*db/db*) mice. The effects of decreasing glucose from 2.5 to 0.1 mM on VMH GE neurones were similar in wild-type and *db/db* mice. However, decreasing glucose from 2.5 to 0.5 mM decreased the action potential frequency, membrane potential and input resistance of VMH GE neurones to a significantly greater extent in *db/db* versus wild-type mice. Furthermore, insulin (5 nM) blunted the effects of decreased glucose in wild-type, but not *db/db* mice. These differences in both glucose and insulin sensitivity between wild-type and *db/db* mice were completely ameliorated by the insulin sensitiser, Compound 2 (300 nM). These data are consistent with our hypothesis that impaired insulin signalling in T2DM sensitises VMH GE neurones to decreased glucose.

The ventromedial hypothalamus (VMH), which consists of the ventromedial (VMN) and arcuate (ARC) nuclei, plays a critical role in the regulation of energy and glucose homeostasis (1, 2). The VMH contains neurones whose activity is regulated by changes in extracellular glucose (3, 4). Glucose-excited (GE) neurones increase and glucose-inhibited (GI) neurones decrease their activity as extracellular glucose increases (3). Insulin regulates both VMH GE and GI neurones (5, 6). Mice with a neurone-specific disruption of the insulin-receptor gene (NIRKO mice) exhibit increased food intake, body weight and insulin resistance, consistent with type 2 diabetes mellitus (T2DM) (7). Furthermore, NIRKO mice do not increase epinephrine and norepinephrine in response to decreased circulating glucose levels (8). These results suggest that dysfunctional insulin signalling in the central nervous system impairs energy and glucose homeostasis. VMH glucose sensing neurones are impaired when central nervous system responses to hypoglycaemia are impaired

(9, 10). Moreover, VMH GE neurones are refractory to the effects of insulin during T2DM (11). Thus, it is plausible that the central nervous system effects of insulin on energy and glucose homeostasis may be mediated, in part, through VMH glucose sensing neurones.

We recently demonstrated that insulin attenuates the response of VMH GE neurones to decreased glucose (12). The effect of insulin on the glucose sensitivity of VMH GE neurones is mediated by the phosphoinositol-3-kinase (PI3K) signalling pathway (12). This is consistent with earlier reports that PI3K mediates the central nervous system effects of insulin on food intake as well as on the activity of VMH GE neurones (11, 13). Insulin resistance during T2DM is associated with an impairment of the hypothalamic PI3K signalling pathway (14, 15). Thus, we hypothesise that the response of VMH GE neurones to decreased glucose will be enhanced in T2DM as a result of dysfunctional PI3K signalling. Furthermore, restoration of the PI3K signalling pathway in GE neurones with the

insulin sensitiser Compound 2 (300 nM) (16, 17) will normalise their glucose sensitivity. Compound 2 reduces plasma glucose and insulin levels in diabetic rodent models and potentiates the effects of insulin via enhancing PI3K activity (16–19). We test our hypothesis using patch-clamp recordings of VMH GE neurones in brain slices in the diabetic *db/db* mouse.

Materials and methods

Preparation of brain slices

All procedures were approved by the Institutional Animal Care and Use Committee (IACUC) at the New Jersey Medical School. Male 35–42-day-old C56Bl/6 (wild-type) and *db/db* mice were housed at the New Jersey Medical School (NJMS) animal facility with their dams at 22–23 °C under a 12 : 12 h light/dark cycle. Animals were maintained on Purina Rat Chow 5001 (Ralston-Purina, St Louis, MO, USA) and water was available *ad lib*. On the day of the experiment, mice were anaesthetised with 50 mg/kg pentobarbital and transcardially perfused. Brains were then rapidly removed and placed in an ice cold slushy oxygenated perfusion solution. Sections (300 μm) through the hypothalamus were maintained at 32 °C in oxygenated artificial cerebrospinal fluid (ACSF) composed of (in mM): 126 NaCl, 1.9 KCl, 1.2 KH_2PO_4, 26 $NaHCO_3$, 2.5 glucose, 9 $MgCl_2$, 0.3 $CaCl_2$; osmolarity adjusted to approximately 310 mOsm with sucrose; pH 7.4. Slices were then transferred to normal oxygenated ACSF (2.4 mM $CaCl_2$, 1.3 mM $MgCl_2$) for the remainder of the experiment.

Chemicals

The nonpeptide small-molecule insulin sensitiser Compound 2 was provided by Dr Bei B. Zhang (Merck Research Laboratories, Rahway, NJ, USA). A stock solution of 20 mM Compound 2 (FW: 345 U) was prepared in 100% dimethylsulfoxide (DMSO) (Sigma-Aldrich, St Louis, MO, USA) with ascorbic acid (200 μg/ml) to improve compound stability. The stock solution of Compound 2 was diluted in ACSF to a final concentration of 300 nM Compound 2 in 0.01% DMSO. This concentration of Compound 2 corresponds to the half maximal dose, as previously identified (17). A stock solution of the PI3K inhibitor LY294002 (Sigma) was dissolved in DMSO and diluted in ACSF to a final concentration of 10 μM in 0.01% DMSO. This concentration of LY294002 was previously shown to block the effects of insulin on VMH GI neurones (6).

Electrophysiology: whole-cell recordings in brain slices

Viable neurones were visualised and studied under infrared differential-interference contrast microscopy using a Leica DMLFS microscope (Leica Microsystems, Wetzlar, Germany Leica Microsystems, Wetzlar, Germany) equipped with a × 40 long-working-distance water-immersion objective. Current- and voltage-clamp recordings from neurones with in the ventrolateral (VL)-VMN neurones were performed using an Axopatch-1D amplifier (Axon Instruments, Foster City, CA, USA). We have previously shown that VMH GE neurones are selectively located in the VL-VMN (12). Data were simultaneously digitised at 5 kHz (Digidata 1320A; Axon Instruments) and analysed using pCLAMP 9.2 software (Molecular Devices, Foster City, CA, USA). During recording, brain slices were perfused at 6 ml/min with normal oxygenated ACSF. Borosilicate pipettes (1.4–3.5 MΩ; Sutter Instruments, Novato, CA, USA) were filled with an intracellular solution containing (in mM): 128 K-gluconate, 10 KCl, 4 KOH, 10 HEPES, 4 $MgCl_2$, 0.5 $CaCl_2$, 5 ethylene glycol tetraacetic acid; pH 7.2. Osmolarity was adjusted to 290–300 mOsm with sucrose. Amphotericin-B was included in

the patch pipette to establish the perforated patch recording configuration (final concentration 240 μg/ml, stock 60 mg/ml DMSO). The junction potential between the bath and the patch pipette was nulled before the formation of a gigaohm seal. The liquid junction potential was calculated to be 10 mV using pClamp 9.2 and the data were adjusted offline. The membrane potential and action potential frequency were allowed to stabilise for 10–15 min after the formation of a gigaohm seal to allow for the amphotericin-B to perforate the membrane. Neurones whose access resistance exceeds 40 M were rejected. Input resistance was calculated from the change in membrane potential in response to small 500 ms hyperpolarising pulses (-10 to -20 pA) given every 3 s, as described previously (3, 5). The reversal potential was calculated from the change in membrane current in response to voltage steps from -120 mV to $+60$ mV from a holding potential of -60 mV. Steady-state currents were determined by measuring data points within the last 5 ms of the 200-ms voltage pulses. GE neurones are identified as those that reversibly decrease their action potential frequency, membrane potential and input resistance with a decrease in extracellular glucose from 2.5 to 0.1 mM. A glucose concentration of 2.5 mM represents the physiological glucose concentration normally seen in the VMH in the fed state (20, 21). A maximal decrease to 0.1 mM enables us to reliably identify GE neurones and provides a stable reference for calculating percent change in response. The glucose sensitivity of GE neurones was evaluated using glucose decreases from 2.5 to 0.1 or 0.5 mM in the absence or 10 min after the addition of insulin, compound 2 and/or LY294002. The data are expressed as percent change as a result of variability between neurones as described previously (3, 5, 10, 12, 22, 23).

Western blot analysis

The VMH was dissected from 300 μM slices made through the hypothalamus and placed in oxygenated ACSF. VMH sections were exposed for 10 min to the treatments described in the Results to maintain consistency with electrophysiological recordings. Sections were then homogenised in RIPA buffer (50 mM Tris–HCl, 1% NP-40, 0.25% Na deoxycholate, 150 mM NaCl, 1 mM ethylenediaminetetraacetic acid, 1 mM phenylmethylsulphonyl fluoride, 1 μg/ml leupeptin, 21 μg/ml aprotinin, 1 μg/ml pepstatin A) at 4 °C. Lysate supernatant was collected (10 min at 14 000 g at 4 °C) and frozen at -80 °C. Protein (30 μg; determined by a modified Bradford Assay) was loaded on a 12% Tris–HCl gel (Pierce, Rockford, IL, USA) and electrophoresed for 65 min at 120 V. Proteins were transferred to nitrocellulose membranes (Bio-Rad, Hercules, CA, USA) for 1 h at 350 mA. Immunodetection was performed overnight at 4 °C using rabbit polyclonal antibodies against anti phospho-atypical protein kinase ser473 (pAkt, dilution 1 : 10 000; Cell Signaling #4051, Danvers, MA, USA), or β-actin (1 : 10 000; dilution Sigma). Membranes were then incubated with a biotinylated IgG (H + L) antibody (anti-rabbit dilution 1 : 10 000; Vector, Torrance, CA, USA) for 1 h at room temperature. Membranes were finally incubated with a horseradish peroxidase-strepdavin (Peirce, Rockford, IL, USA) antibody for 90 min at room temperature before signals were visualised using the SuperSignal West Pico ECL kit (Thermo Scientific, Rockford, IL, USA). Western blots were imaged on a Bio-Rad ChemDoc XRS (Bio-Rad). Quantification was performed using ImageQuant (GE Healthcare, Niskayuna, NY, USA). The results are presented as the percentage of control after normalisation to β-actin.

Statistical analysis

All data are expressed as the mean $\pm$ SE. Statistical analysis was performed using Student's *t*-test or one-way analysis of variance (ANOVA). P < 0.05 was considered statistically significant.

Results

The average blood glucose level in the 4–5-week-old *db/db* mice was significantly greater than that of the wild-type mice (*db/db*: 217.3 ± 11.9 mg/dl; wild-type: 157.5 ± 4.7 mg/dl; P < 0.00001). On the basis of our previous findings showing that GE neurones are concentrated in the VL-VMN, we focused on GE neurones located within this region (5, 12). A total of 182 VL-VMN neurones were evaluated using whole-cell patch clamp recordings. Of the 93 VL-VMN neurones recorded from wild-type (C57Bl/6) mice, 18 (19%) were GE neurones. A similar percentage of GE neurones were found in the VL-VMN of *db/db* mice (16 of 89 neurones; 18%). These 34 GE neurones from wild-type and *db/db* mice were then used for subsequent experiments. Thus, all experiments were performed in VL-VMN GE neurones. However, not all recordings could be maintained for a sufficient time to allow all experi-

mental manipulations to be performed on each GE neurone. VL-VMN GE neurones from wild-type and *db/db* mice did not differ in baseline (i.e. in 2.5 mM glucose) action potential frequency (wild-type: 1.30 ± 0.38 Hz, n = 18; *db/db*: 1.82 ± 0.36 Hz, n = 16; P > 0.05), membrane potential (wild-type: −49.0 ± 1.8 mV, n = 18; *db/db*: −49.2 ± 1.8 mV, n = 16; P > 0.05) or input resistance (wild-type: 350 ± 59 MΩ, n = 17; *db/db*: 357 ± 65 MΩ, n = 16; P > 0.05).

Glucose concentration–response relationship for VL-VMN GE neurones from wild-type mice

Although we previously determined the glucose concentration–response relationship for VL-VMN GE neurones from rats (5, 6), this relationship has not been evaluated for VL-VMN GE neurones from mice. Figure 1(A) shows a continuous whole cell current clamp
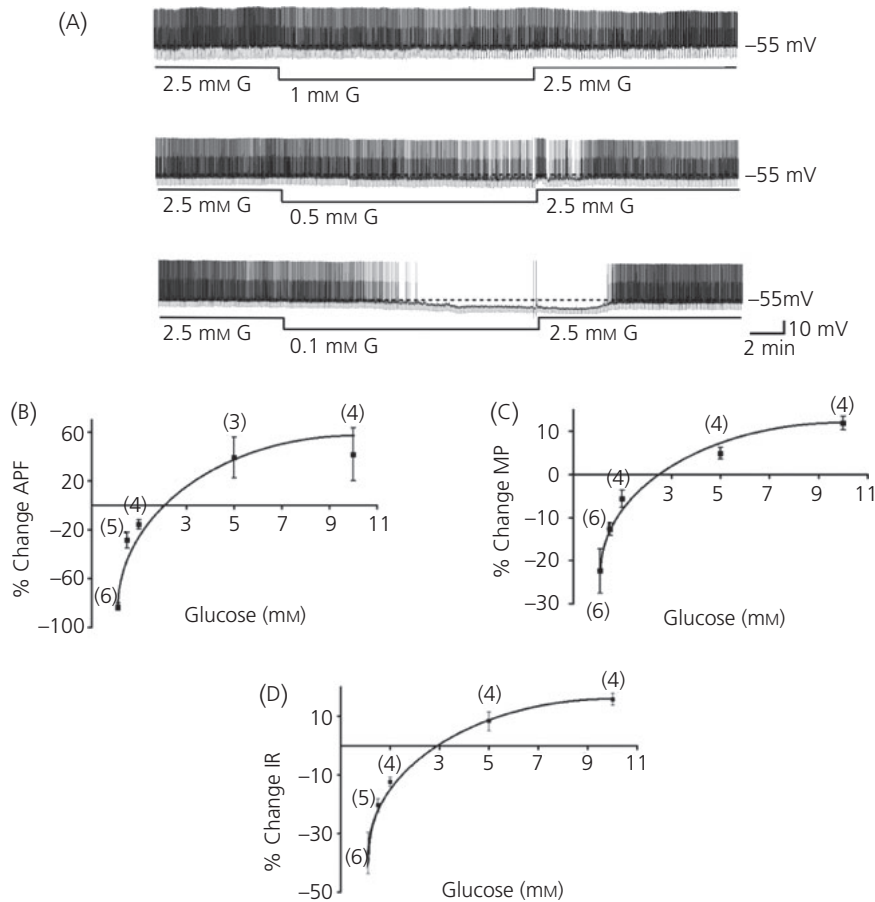

Fig. 1. Concentration–response relationship of ventrolateral-ventromedial (VL-VMN) glucose-excited (GE) neurones in brain slices from wild-type mice to physiological alterations in extracellular glucose. (A) Consecutive current-clamp recordings of spontaneous electrical activity in a VL-VMN GE neurone from a wild-type mouse in response to extracellular glucose concentration decreases from 2.5 mM to 1.0, 0.5 and 0.1 mM. The resting membrane potential in 2.5 mM glucose is given to the right of each trace and indicated by a dotted line. Downward deflections represent the membrane potential response to a constant hyperpolarising current pulse. The membrane voltage response is directly proportional to the change in input resistance. Because of variation between neurones, values are expressed as the percent change in (B) action potential frequency (APF), (C) membrane potential (MP), (D) input resistance (IR) compared to 2.5 mM glucose. Data points represent the mean ± standard error. The data fit the equation for a rectangular hyperbole: %change = [E_{max} × (glucose)]/[EC_{50} + (glucose)] + i, where i is a constant that does not force the rectangular hyperbole to pass through origin. The EC_{50} for APF, MP and IR was 1.59 mM, 1.04 mM and 1.63 mM, respectively.

(A) Wild-type

2.5 mm G   0.5 mm G   2.5 mm G   −49 mV

2.5 mm G + Cmpd 2   0.5 mm G + Cmpd 2   2.5 mm G + Cmpd 2   −49 mV   10 mV / 2 min

(B) *db/db*

2.5 mm G   0.5 mm G   2.5 mm G   −55 mV

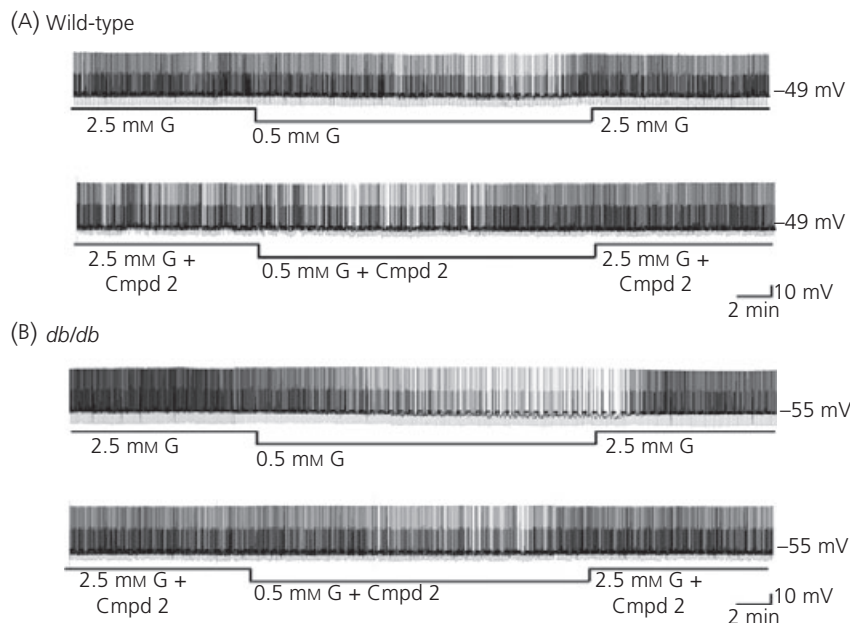2.5 mm G + Cmpd 2   0.5 mm G + Cmpd 2   2.5 mm G + Cmpd 2   −55 mV   10 mV / 2 min

Fig. 2. Consecutive current-clamp recordings of spontaneous electrical activity in ventrolateral-ventromedial (VL-VMN) glucose-excited (GE) neurones from wild-type (A) and *db/db* (B) mice. The resting membrane potential in 2.5 mm glucose is given to the right of each trace and indicated by a dotted line. Downward deflections represent the membrane potential response to a constant hyperpolarising current pulse. The membrane voltage response is directly proportional to the change in input resistance. (A) Decreasing extracellular glucose from 2.5 to 0.5 mm hyperpolarised and decreased action potential frequency in this VL-VMN GE neurone from a wild-type mouse. Compound 2 (300 nm) had no effect on the activity of this VL-VMN GE neurone in 2.5 mm glucose, nor did it alter glucose sensitivity. (B) The inhibitory effect of decreased glucose from 2.5 to 0.5 mm is more pronounced in this VL-VMN GE neurone from a *db/db* mouse. Compound 2 had no effect on neuronal activity in 2.5 mm glucose; however, it restored glucose sensitivity to that seen in the wild-type.

recording from a VL-VMN GE neurone in response to glucose concentration decreases from 2.5 to 1.0, 0.5 and 0.1 mm. The magnitude of the decrease in action potential frequency increases with the magnitude of the glucose decrease. The action potential frequency (Fig. 1b), membrane potential (Fig. 1c) and input resistance (Fig. 1d) of VL-VMN GE neurones from wild-type mice show concentration-dependent responses to changes in extracellular glucose within the physiological range. The relationship between extracellular glucose concentration and electrophysiological parameters of neuronal activity (action potential frequency, membrane potential and input resistance) was well fit by a rectangular hyperbole, with the steepest slope occurring over a concentration range of glucose of 0.1–2 mm. The response of VL-VMN GE neurones to an increasing glucose concentration reached a plateau at 5 mm. The half maximal effective concentration of glucose (EC_{50}) was calculated to be 1.59 mm for action potential frequency, 1.04 mm for membrane potential, and 1.63 mm for input resistance (Fig. 1) (24). These results were similar to those previously reported for GE neurones in rats (5, 12).

The response of VL-VMN GE neurones to decreased glucose is enhanced in *db/db* mice

Decreasing extracellular glucose from 2.5 to 0.5 mm decreased the action potential frequency of VL-VMN GE neurones from *db/db* mice to a significantly greater extent than that seen in wild-type mice (*db/db*: 51.5%, n = 10; wild-type: 20.9 ± 2.5%, n = 6;

$P < 0.05$; Figs 2 and 3). Similar results were observed for membrane potential and input resistance (Fig. 3). There was no significant difference in action potential frequency, membrane potential or input resistance of GE neurones from wild-type or *db/db* mice when Compound 2 (300 nm) was added to 2.5 mm glucose ($P > 0.05$ for all variables; Fig. 2). Compound 2 had no effect on the glucose sensitivity of VL-VMN GE neurones from wild-type mice. However, Compound 2 reduced the magnitude of the decrease in action potential frequency, membrane potential and input resistance of VL-VMN GE neurones from *db/db* mice in response to decreased glucose from 2.5 to 0.5 mm to that seen in the wild-type mice (Figs 2 and 3). There was no significant difference between GE neurones from wild-type and *db/db* mice in response to a maximal glucose decrease. Decreasing glucose from 2.5 to 0.1 mm decreased the action potential frequency of VL-VMN GE neurones by 78.4 ± 5.6% (n = 18) in wild-type and 74.4 ± 5.9% (n = 16; $P > 0.05$) in *db/db* mice. Similar results were seen for the percent change in membrane potential (wild-type: −24.4 ± 2.9%, n = 16, *db/db*: −26.8 ± 3.5%, n = 14; $P > 0.05$) and input resistance (wild-type: −34.5 ± 2.0%, n = 17, *db/db*: −37.9 ± 3.3%, n = 14; $P > 0.05$).

VL-VMN GE neurones from *db/db* mice are refractory to the effects of insulin on glucose sensitivity

To compare the effects of insulin on the glucose sensitivity of VL-VMN GE neurones from wild-type and *db/db* mice, we used a
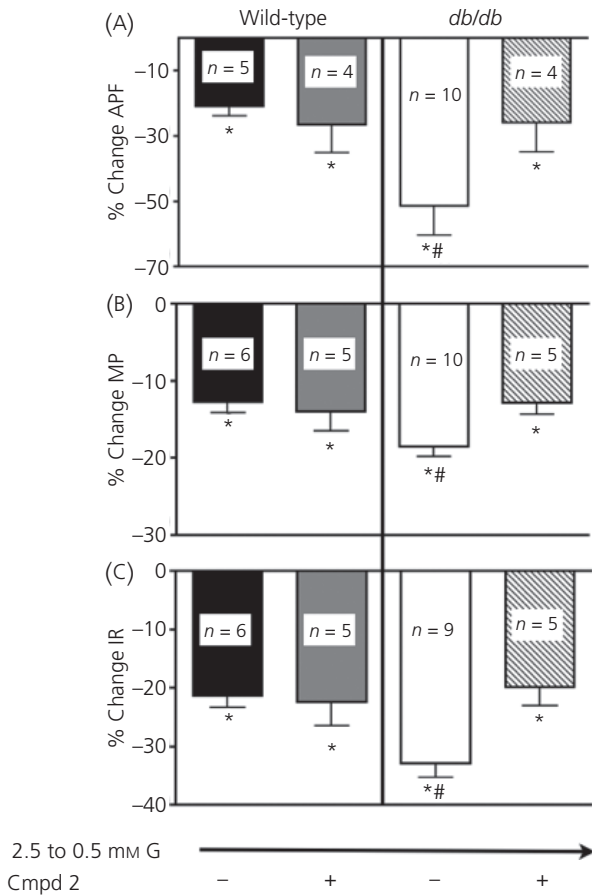
Fig. 3. Decreasing extracellular glucose (G) from 2.5 to 0.5 mM decreased action potential frequency (A; APF), membrane potential (B; MP) and input resistance (C; IR) to a greater extent in *db/db* compared to wild-type (WT) mice (white versus black bars). Decreasing glucose from 2.5 to 0.5 mM in the presence of Compound 2 (Cmpd2, 300 nM), decreased APF IR, and MP to an equal extent in VL-VMN GE neurones from wild-type (n = 5) and *db/db* (n = 5) mice (grey versus stripped bars). *P < 0.05 compared to no change; #P < 0.05 wild-type versus *db/db*.

glucose concentration decrease that inhibited GE neurones in both genotypes to a similar degree (e.g. 2.5 to 0.1 mM). The top trace of Fig. 4(A) illustrates the normal decrease in action potential frequency of VL-VMN GE neurones from wild-type mice in response to decreased glucose from 2.5 to 0.1 mM. This is accompanied by a significant decrease in membrane potential and input resistance (Fig. 5A). As observed for rats (12), the response of VL-VMN GE neurones from wild-type mice to decreased glucose is significantly attenuated in the presence of insulin (Fig. 4A, bottom trace; Fig. 5A). However, VL-VMN GE neurones from *db/db* mice were refractory to the effects of insulin on glucose sensitivity (Fig. 4B; top two traces). When glucose was lowered from 2.5 to 0.1 mM in the presence and absence of 5 nM insulin, the action potential frequency of VL-VMN GE neurones from *db/db* mice was not significantly different (with insulin: −79.4 ± 9.3%; without insulin: −74.4 ± 5.3%; n = 6 P < 0.05). Similar results were seen with input resistance and membrane potential (Fig. 5B).

As shown above for the glucose sensitivity of VL-VMN GE neurones from *db/db* mice, Compound 2 also restored the effects of insulin on glucose sensitivity to these neurones (Fig. 4B, third trace; Fig. 5). Thus, when glucose was lowered from 2.5 to 0.1 mM in the presence of insulin and Compound 2 (300 nM), the action potential frequency of VL-VMN GE neurones from *db/db* mice was significantly attenuated compared to that observed in the absence of Compound 2 when glucose was lowered alone or in the presence of insulin (decreased glucose with insulin/Compound 2: −29.4 ± 6.3%; n = 5; decreased glucose alone: 74.5 ± 5.9%, n = 16; decreased glucose with insulin: −79.4 ± 9.3%, n = 6; P < 0.05; Fig. 4B, top 3 traces; Fig. 5B). Furthermore, the decrease in action potential frequency of VL-VMN GE neurones from *db/db* mice in response to decreased glucose in the presence of insulin and Compound 2 was similar to that of wild-type mice in the presence of insulin alone (Fig. 4). Similar results were seen for membrane potential and input resistance (Fig. 5A, B). Finally, Compound 2 had no effect on the change in action potential frequency, membrane potential and input resistance of VL-VMN GE neurones from wild-type mice in response to decreased glucose (Fig. 5A).

The effects of Compound 2 on VL-VMN GE neurones from *db/db* mice were blocked by the PI3K inhibitor LY294002 (10 μM; Fig. 4B, bottom trace; Fig 5B). When glucose was decreased from 2.5 to 0.1 mM in the presence of insulin, Compound 2 (300 nM) and LY294002 the action potential frequency of VL-VMN GE neurones from *db/db* mice was decreased by 75.4 ± 9.1% (n = 5). This was not significantly different from the decrease in action potential frequency of VL-VMN GE neurones from *db/db* mice observed when glucose was decreased either alone (−74.5 ± 5.9, n = 16) or in the presence of insulin (−79.4 ± 9.3; n = 6, P > 0.05; Figs 4B and 5B). Similar results were observed for membrane potential and input resistance (Fig. 5B). The current–voltage relationship for insulin in 2.5 mM glucose in VL-VMN GE neurones from *db/db* mice did not intersect with that obtained in 2.5 mM glucose over the voltage range tested as expected because there were no effects of insulin on the input resistance of these neurones (Fig. 6). However, in the presence of Compound 2, the insulin-induced current reversed at −85 ± 5 mV (n = 4). This reversal potential is near the theoretical potassium equilibrium potential in our solutions (−99 mV; Fig. 6).

Finally, to verify that the effects of Compound 2 and LY294002 on the glucose sensitivity of VL-VMN GE neurones were via the PI3K signalling pathway, we measured the phosphorylation level of the downstream target of PI3K, atypical protein kinase (Akt) in the VMH. Figure 7(A, B) shows representative immunoblots for treated VMH sections run on the same membranes for comparison. Average values for pAkt expressed relative to *β*-actin are shown in Fig. 7(C). VMH sections were exposed to the various treatments for 10 min for consistency with electrophysiological recordings. There were no significant differences in baseline VMH Akt phosphorylation between wild-type and *db/db* mice. Insulin significantly increased pAKt phosphorylation in the wild-type but not the *db/db* mice. Compound 2 (300 nM) increased insulin-stimulated VMH pAkt levels in *db/db* mice to the levels seen in the wild-type. There was no significant effect of Compound 2 alone on VMH pAkt levels in the wild-type; however Compound 2 increased pAkt levels in the *db/db*
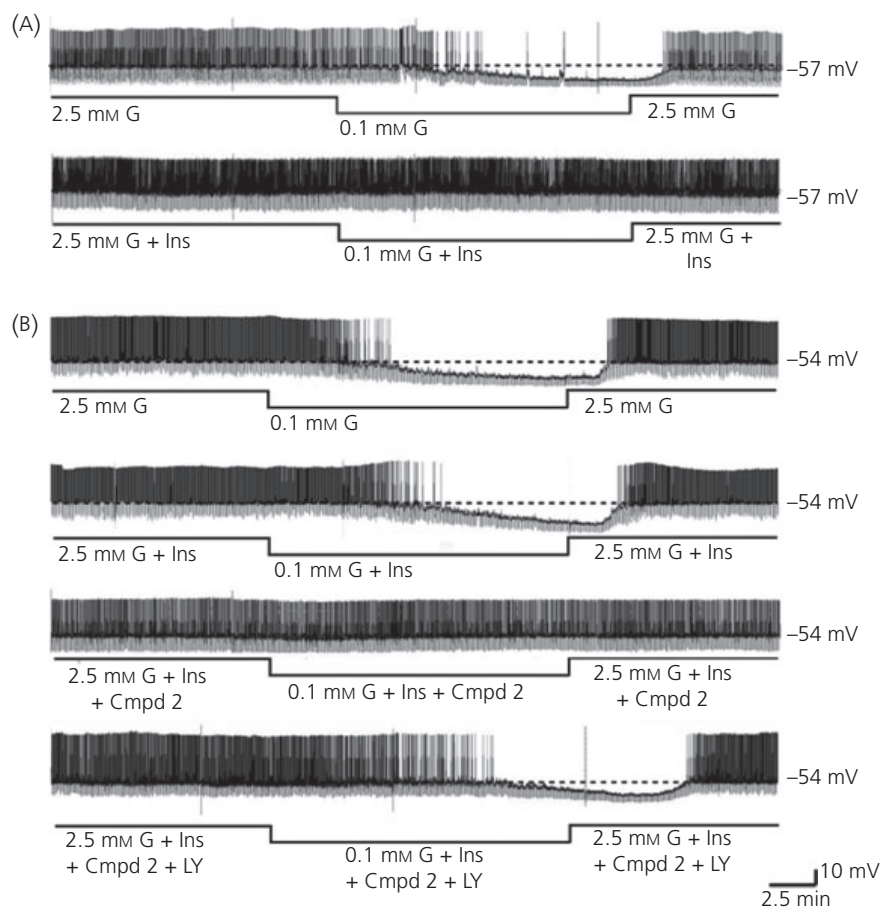
Fig. 4. Continuous consecutive whole-cell current clamp recordings of spontaneous electrical activity in a ventrolateral-ventromedial (VL-VMN) glucose-excited (GE) neurone in wild-type (WT, A) and *db/db* (B) mice. The resting membrane potential is indicated by the horizontal dotted line and noted at the right of each trace. Downward deflections represent the membrane voltage response to a constant hyperpolarising pulse. The membrane voltage response is directly proportional to the change in input resistance. (A) Decreasing extracellular glucose (G) levels from 2.5 to 0.1 mM in wild-type mice causes decreased input resistance and decreased action potential frequency (A; top[t] trace). The response to decreased glucose is reduced in the presence of 5 nM insulin (Ins, A: bottom trace). (B) Decreasing extracellular glucose levels from 2.5 to 0.1 mM in *db/db* mice causes hyperpolarisation, decreased input resistance and decreased action potential frequency (B: top trace). Insulin (Ins) had no effect on the response of VL-VMN GE neurones from *db/db* mice to decreased glucose (B; second trace). The insulin sensitiser, (Cmpd 2; 300 nM), restored the effects of insulin (Ins) in the *db/db* mice (B; third trace). The effects of Compound 2 were blocked by administration of the PI3K inhibitor, LY294002 (LY, 10 μM, B; bottom trace).

mice. Finally, the PI3K inhibitor, LY294002 blocked the effects of insulin and Compound 2 in both wild-type and *db/db* mice.

Discussion

The present study is the first to demonstrate that the glucose sensitivity of VL-VMN GE neurones is altered in a murine model of early T2DM. Moreover, glucose sensitivity is dependent on the PI3K signalling pathway. That is, the response of VL-VMN GE neurones from *db/db* mice to decreased glucose is enhanced compared to that in wild-type mice. VL-VMN GE neurones from *db/db* mice are also refractory to the effects of insulin on glucose sensitivity. When insulin sensitivity is enhanced via the IRS-PI3K signalling pathway, the glucose sensitivity of VL-VMN GE neurones from *db/db* mice is restored to that observed in wild-type mice. These data suggest

that functional IRS-PI3K signalling is critical for normal central glucose sensing.

Impaired PI3K signalling underlies insulin resistance in T2DM (14, 15). The phosphorylation of several key downstream effectors of PI3K (e.g. PKB/Akt, p85α) is reduced in *db/db* mice (25, 26). The small-molecule insulin sensitiser, Compound 2 activates the insulin receptor (16, 17) and phosphorylates PKB/Akt, leading to increased glucose uptake and a significant reduction in plasma glucose levels in these mice (16, 17, 19). Compound 2 also significantly decreases food intake and body weight in *db/db* mice (17). The effects of Compound 2 on plasma glucose levels and food intake were inhibited by the PI3K inhibitor wortmannin (17). We showed previously that PI3K mediates insulin-induced attenuation of the response of VL-VMN GE neurones to decreased glucose (12). The current data indicate that Compound 2 restores both basal and insulin-regulated
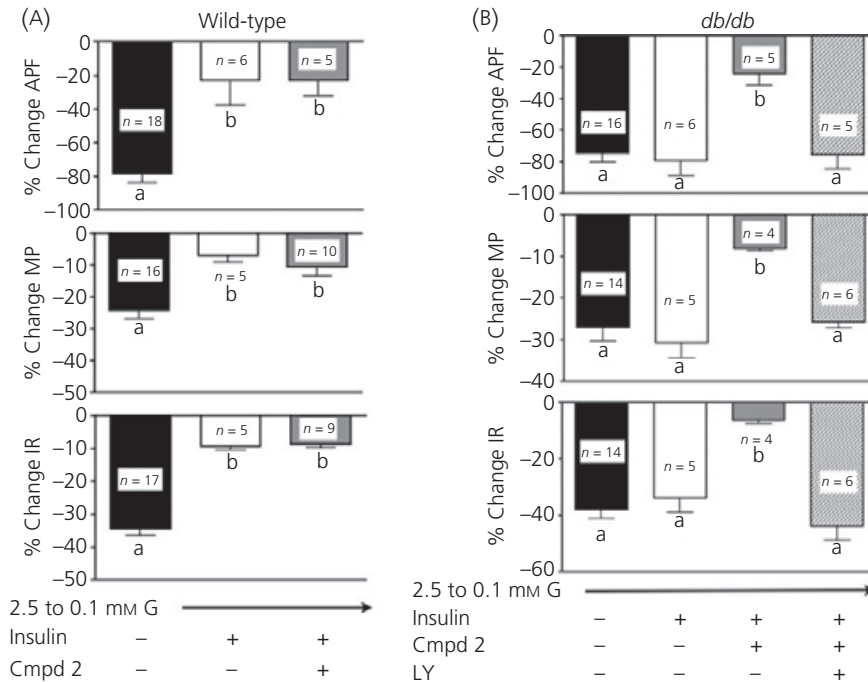
Fig. 5. (A) Wild-type mice: Decreasing extracellular glucose (G) from 2.5 to 0.1 mm in the presence of insulin significantly attenuated the decrease in action potential frequency (APF; top), membrane potential (MP; middle) and input resistance (IR; bottom) associated with a decrease in extracellular glucose alone in wild-type mice (black versus white bars). Administration of the insulin sensitiser Compound 2 (Cmpd2, 300 nm) had no effect on glucose sensitivity in GE neurones from wild-type (WT) mice (grey bar). (B) db/db mice: The effect of decreased extracellular glucose from 2.5 to 0.1 mm on VL-VMN GE neurones from db/db mice was similar in the presence and absence of insulin (black and white bars). Administration of Compound 2 (grey bar) restored insulin sensitivity in these animals, significantly blunting the decrease in action potential frequency (APF; top), membrane potential (MP; middle) and input resistance (IR; bottom). The effects of Compound 2 were blocked via administration of the PI3K inhibitor LY294002 (LY, 10 μm; striped bar). Bars with different letters are statistically different (P < 0.05).
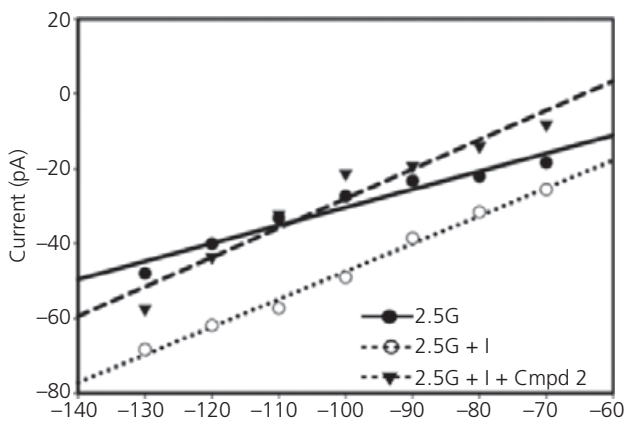

Fig. 6. Current–voltage relationships in a ventrolateral-ventromedial glucose-excited neurone from a db/db mouse. The current–voltage relationship for insulin in 2.5 mm glucose (G) does not intersect that obtained in 2.5 mm glucose alone over the voltage range tested. However, when insulin (Ins) was added to 2.5 mm glucose in the presence of Compound 2 (Cmpd2), the insulin sensitive conductance reverses near the theoretical K$^+$ equilibrium potential of −90 mV.

glucose sensitivity in VL-VMN GE neurones from db/db mice. Compound 2 also appears to restore insulin effects on the KATP channel in these neurones because the insulin-induced current reversed at

the K$^+$ equilibrium potential in the presence but not the absence of Compound 2. As predicted, both our electrophysiological experiments as well as immunoblots of Akt phosphorylation show that the effects of Compound 2 on the glucose sensitivity of VL-VMN GE neurones are dependent on the PI3K signalling pathway. Collectively, these data suggest that normal central glucose sensing, at least by VL-VMN GE neurones, is dependent on normal insulin sensitivity and activity of the PI3K signalling pathway. Moreover, these data provide support for a link between dysfunctional glucose sensing in VL-VMN GE neurones and T2DM.

Although Compound 2 enhances PI3K signalling, it had no effect on the glucose sensitivity of VL-VMN GE neurones from wild-type mice. Nor did Compound 2 increase VMH pAkt phosphorylation in the wild-type mice. This is consistent with the study by Qureshi et al. (17) who found that Compound 2 attenuated the hyperglycaemia of db/db mice but had no effect on blood glucose levels in wild-type mice. Moreover, Compound 2 did not lower blood glucose levels in a rodent model of type 1 diabetes mellitus unless coadministered with insulin (17). Thus, although an insulin-mimetic action of Compound 2 has been reported at higher concentrations, our data are consistent with the predominantly insulin-sensitising effects of Compound 2 seen at lower concentrations of this drug in nondiabetic animals (16, 17).
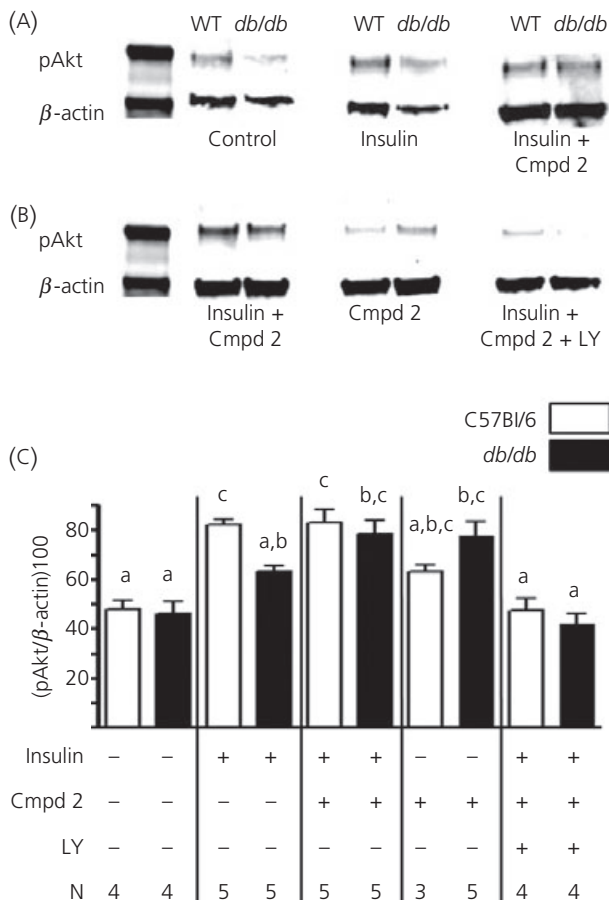
Fig. 7. (A, B) Representative immunoblots of phosphorylated atypical protein kinase (pAkt) and β-actin in ventromedial hypothalamus (VMH) tissue from wild-type (WT) and *db/db* mice. (A, B) Data from immunoblots run on the same membranes for comparison. (C) Averages of VMH pAkt levels expressed relative to β-actin. Insulin significantly increased VMH pAkt levels in the wild-type but not the *db/db* mice. Compound 2 (Cmpd 2, 300 nM) had no effect in the wild-type mice; however, it increased basal and insulin-stimulated VMH pAkt in the *db/db* mice to that levels seen in the insulin-stimulated VMH from wild-type mice. The PI3K inhibitor, LY294002 (LY, 10 μM) blocked the effects of Compound 2. N values are given below each bar. Bars with different letters are statistically different ($P < 0.05$).

One caveat is that we cannot conclude in our studies that insulin resistance *per se* is sufficient to explain the decreased glucose sensitivity of VL-VMN GE neurones. This is because PI3K also mediates leptin-induced KATP channel activation in GE neurones (27). The *db/db* mice exhibit a homozygous mutation of the leptin receptor resulting in leptin resistance (28). While Compound 2 increases phosphorylation of insulin receptor subunits, it also stimulates PI3K signalling (e.g. Akt phosphorylation) downstream of the insulin and leptin receptors (16, 17; present study). Therefore, we do not know whether the primary defect in glucose sensing by VL-VMN neurones from *db/db* mice results from insulin or leptin resistance. It is also possible that synergistic modulation of VL-VMN GE neurones by both insulin and leptin is required for normal glucose sensitivity. These issues could be more definitively resolved using a model of

dietary obesity and T2DM lacking the leptin receptor mutation. However, young, 4–6-week-old animals are necessary to perform the long patch clamp recordings required to measure the glucose sensitivity of VL-VMN GE neurones. It is well established that *db/db* mice are significantly hyperinsulinaemic at 4–5 weeks of age (29–32). They are also overweight and hyperleptinaemic (29, 30, 32, 33). Some studies report that hyperglycaemia in *db/db* mice develops between 5 and 8 weeks of age (30, 32), whereas others indicate that these mice are already hyperglycaemic by 4–5 weeks of age (29, 31). Importantly, the *db/db* mice used in the present study were significantly, albeit mildly, hyperglycaemic at an age where hyperinsulinaemia is well known, suggesting the appearance of early insulin resistance. There are no dietary models of T2DM that reach a sufficient level of insulin resistance at this age. However, the take home message remains the same regardless of animal model. Impaired PI3K signalling as a result of insulin and/or leptin resistance in T2DM enhances the response of VL-VMN GE neurones to decreased glucose.

The physiological significance of enhanced responses of VL-VMN GE neurones to decreased glucose during T2DM is still purely speculative. In a previous study, we showed that insulin prevented VL-VMN GE neurones from healthy rats from being inhibited by decreased extracellular glucose from 2.5 to 0.5 mM (12). This glucose decrease is analogous to that seen in the VMH after an overnight fast (34). Thus, in the presence of insulin, VL-VMN GE neurones would not be inhibited by decreases in extracellular glucose associated with circadian or meal to meal fluctuations. Rather, the activity of VL-VMN GE neurones would only be silenced by decreases in glucose that might occur during a severe glucose deficit (e.g. hypoglycaemia). This is consistent with the role of insulin as a satiety factor in the brain (13). However, this attenuating effect of insulin is released during T2DM allowing the activity of VL-VMN GE neurones to be regulated by small daily glucose fluctuations. Thus, one might further speculate that during T2DM the brain might perceive glucose deficit under conditions of energy sufficiency (or even excess), possibly contributing to over-activation of energy conserving mechanisms. However, we are clearly still a long way from assigning a physiological role to VL-VMN GE neurones in health as well as in T2DM.

In conclusion, insulin attenuates the response of VL-VMN GE neurones to decreased glucose via activation of the PI3K signalling pathway. Conversely, impaired PI3K signalling in T2DM enhances the response of VL-VMN GE neurones to decreased glucose, resulting in the inhibition of neuronal activity in glucose concentrations where they would normally be active. Therefore, abnormal responses of VL-VMN GE neurones to changes in glucose may underlie, in part, the altered central regulation of energy homeostasis in T2DM. Furthermore, normalisation of PI3K signalling normalises glucose and energy homeostasis in T2DM and glucose sensitivity of VL-VMN GE neurones. Thus, the PI3K signalling pathway is a target for therapeutic intervention in T2DM. However, caution must be exercised when attempting to blunt the response of GE neurones to glucose decreases. GE neurones have been implicated in the response of the brain to hypoglycaemia (35). The challenge will be to block the response of VL-VMN GE neurones to small glucose

decreases at the same time as leaving their response to severe glucose deficit intact.

Acknowledgements

References

1 King BM. The rise, fall, and resurrection of the ventromedial hypothalamus in the regulation of feeding behavior and body weight. *Physiol Behav* 2006; **87**: 221–244.

2 Borg WP, During MJ, Sherwin RS, Borg MA, Brines ML, Shulman GI. Ventromedial hypothalamic lesions in rats suppress counterregulatory responses to hypoglycemia. *J Clin Invest* 1994; **93**: 1677–1682.

3 Song Z, Levin BE, McArdle JJ, Bakhos N, Routh VH. Convergence of pre- and postsynaptic influences on glucosensing neurons in the ventromedial hypothalamic nucleus. *Diabetes* 2001; **50**: 2673–2681.

4 Oomura Y, Ono H, Ooyama H, Wayner MJ. Glucose and osmosensitive neurons of the rat hypothalamus. *Nature* 1969; **222**: 282–284.

5 Wang R, Liu X, Hentges ST, Dunn-Meynell AA, Levin BE, Wang W, Routh VH. The regulation of glucose-excited neurons in the hypothalamic arcuate nucleus by glucose and feeding-relevant peptides. *Diabetes* 2004; **53**: 1959–1965.

6 Canabal DD, Song Z, Potian JG, Beuve A, McArdle JJ, Routh VH. Glucose, insulin and leptin signaling pathways modulate nitric oxide (NO) synthesis in glucose-inhibited (GI) neurons in the ventromedial hypothalamus (VMH). *Am J Physiol Regul Integr Comp Physiol* 2006; **292**: R1418–R1428.

7 Bruning JC, Gautam D, Burks DJ, Gillette J, Schubert M, Orban PC, Klein R, Krone W, Muller-Wieland D, Kahn CR. Role of brain insulin receptor in control of body weight and reproduction. *Science* 2000; **289**: 2122–2125.

8 Fisher SJ, Bruning JC, Lannon S, Kahn CR. Insulin signaling in the central nervous system is critical for the normal sympathoadrenal response to hypoglycemia. *Diabetes* 2005; **54**: 1447–1451.

9 McCrimmon RJ, Song Z, Cheng H, McNay EC, Weikart-Yeckel C, Fan X, Routh VH, Sherwin RS. Corticotrophin-releasing factor receptors within the ventromedial hypothalamus regulate hypoglycemia- induced hormonal counterregulation. *J Clin Invest* 2006; **116**: 1723–1730.

10 Song Z, Routh VH. Recurrent hypoglycemia reduces the glucose sensitivity of glucose-inhibited neurons in the ventromedial hypothalamus nucleus (VMN). *Am J Physiol Regul Integr Comp Physiol* 2006; **291**: R1283–R1287.

11 Spanswick D, Smith MA, Mirshamsi S, Routh VH, Ashford MLJ. Insulin activates ATP-sensitive K$^+$ channels in hypothalamic neurons of lean, but not obese rats. *Nat Neurosci* 2000; **3**: 757–758.

12 Cotero VE, Routh VH. Insulin blunts the response of glucose-excited (GE) neurons in the ventrolateral-ventromedial hypothalamic nucleus (VL-VMN) to decreased glucose. *Am J Physiol Endocrinol Metab* 2009; **296**: E1101–E1109.

13 Niswender KD, Morrison CD, Clegg DJ, Olson R, Baskin DG, Myers MG Jr, Seeley RJ, Schwartz MW. Insulin activation of phosphatidylinositol 3-kinase in the hypothalamic arcuate nucleus: a key mediator of insulin-induced anorexia. *Diabetes* 2003; **52**: 227–231.

14 Jiang ZY, Lin YW, Clemont A, Feener EP, Hein KD, Igarashi M, Yamauchi T, White MF, King GL. Characterization of selective resistance to insulin signaling in the vasculature of obese Zucker (*fa*/*fa*) rats. *J Clin Invest* 1999; **104**: 447–457.

15 Niswender KD, Schwartz MW. Insulin and leptin revisited: adiposity signals with overlapping physiological and intracellular signaling capabilities. *Front Neuroendocrinol* 2003; **24**: 1–10.

16 Ding VD, Qureshi SA, Szalkowski D, Li Z, Biazzo-Ashnault DE, Xie D, Liu K, Jones AB, Moller DE, Zhang BB. Regulation of insulin signal transduction pathway by a small-molecule insulin receptor activator. *Biochem J* 2002; **367**: 301–306.

17 Qureshi SA, Ding V, Li Z, Szalkowski D, Biazzo-Ashnault DE, Xie D, Saperstein R, Brady E, Huskey S, Shen X, Liu K, Xu L, Salituro GM, Heck JV, Moller DE, Jones AB, Zhang BB. Activation of insulin signal transduction pathway and anti-diabetic activity of small molecule insulin receptor activators. *J Biol Chem* 2000; **275**: 36590–36595.

18 Air EL, Strowski MZ, Benoit SC, Conarello SL, Salituro GM, Guan XM, Liu K, Woods SC, Zhang BB. Small molecule insulin mimetics reduce food intake and body weight and prevent development of obesity. *Nat Med* 2002; **8**: 179–183.

19 Strowski MZ, Li Z, Szalkowski D, Shen X, Guan XM, Juttner S, Moller DE, Zhang BB. Small-molecule insulin mimetic reduces hyperglycemia and obesity in a nongenetic mouse model of type 2 diabetes. *Endocrinology* 2004; **145**: 5259–5268.

20 Silver IA, Erecinska M. Extracellular glucose concentration in mammalian brain: continuous monitoring of changes during increased neuronal activity and upon limitation in oxygen supply in normo-, hypo-, and hyperglycemic animals. *J Neurosci* 1994; **14**: 5068–5076.

21 Silver IA, Erecinska M. Glucose-induced intracellular ion changes in sugar-sensitive hypothalamic neurons. *J Neurophysiol* 1998; **79**: 1733–1745.

22 Song Z, Routh VH. Differential effects of glucose and lactate on glucosensing neurons in the ventromedial hypothalamic nucleus. *Diabetes* 2005; **54**: 15–22.

23 Wang R, Cruciani-Guglielmacci C, Migrenne S, Magnan C, Cotero VE, Routh VH. The effects of oleic-acid (OA) on distinct populations of neurons in the hypothalamic arcuate nucleus (ARC) are dependent on extracellular glucose levels. *J Neurophysiol* 2005; **55**: 1491–1498.

24 Segel IH. *Enzyme Kinetics*. New York, NY: J. Wiley & Sons, 1975.

25 Niswender KD, Morton GJ, Stearns WH, Rhodes CJ, Myers MG Jr, Schwartz MW. Intracellular signalling key enzyme in leptin-induced anorexia. *Nature* 2001; **413**: 794–795.

26 Shao J, Yamashita H, Qiao L, Friedman JE. Decreased Akt kinase activity and insulin resistance in C57BL/KsJ-Leprdb/db mice. *J Endocrinol* 2000; **167**: 107–115.

27 Spanswick D, Smith MA, Groppi VE, Logan SD, Ashford MLJ. Leptin inhibits hypothalamic neurons by activation of ATP-sensitive potassium channels. *Nature* 1997; **390**: 521–525.

28 Lee GH, Proenca R, Montez JM, Carroll KM, Darvishzadeh JG, Lee JI, Friedman JM. Abnormal splicing of the leptin receptor in diabetic mice. *Nature* 1996; **379**: 632–635.

29 Garris DR. Reproductive tract and pancreatic norepinephrine levels in pre- and overt-diabetic C57BL/KsJ mice: relationship to body weight, blood glucose, serum insulin, and reproductive dysfunction. *Proc Soc Exp Biol Med* 1988; **189**: 79–83.

30 Kodama H, Fujita M, Yamazaki M, Yamaguchi I. The possible role of age-related increase in the plasma glucagon/insulin ratio in the enhanced hepatic gluconeogenesis and hyperglycemia in genetically diabetic (C57BL/KsJ-db/db) mice. *Jpn J Physiol* 1994; **66**: 281–287.

31 Yamanaka M, Itakura Y, Tsuchida A, Nakagawa T, Taiji M. Brain-derived neurotrophic factor (BDNF) prevents the development of diabetes in pre-diabetic mice. *Biomed Res* 2008; **29**: 147–153.

32 Buchanan J, Mazumder PK, Hu P, Chakrabarti G, Roberts MW, Yun UJ, Cooksey RC, Litwin SE, Abel ED. Reduced cardiac efficiency and altered substrate metabolism precedes the onset of hyperglycemia and contractile dysfunction in two mouse models of insulin resistance and obesity. *Endocrinology* 2005; **146**: 5341–5349.

33 Frederich RC, Lollmann B, Hamann A, Napolitano-Rosen A, Kahn BB, Lowell BB, Flier JS. Expression of ob mRNA and its encoded protein in rodents. Impact of nutrition and obesity. *J Clin Invest* 1995; **96**: 1658–1663.

34 De Vries MG, Arseneau LM, Lawson ME, Beverly JL. Extracellular glucose in rat ventromedial hypothalamus during acute and recurrent hypoglycemia. *Diabetes* 2003; **52**: 2767–2773.

35 Miki T, Liss B, Minami K, Shiuchi T, Saraya A, Kashima Y, Horiuchi M, Ashcroft FM, Minokoshi Y, Roeper J, Seino S. ATP-sensitive potassium channels in hypothalamic neurons play an essential role in the maintenance of glucose homeostasis by controlling glucagon release and food intake. *Nat Neurosci* 2001; **5**: 507–512.